


Article

Development of Thiophene Compounds as Potent Chemotherapies for the Treatment of Cutaneous Leishmaniasis Caused by *Leishmania major*

Felipe Rodriguez ¹, Eva Iniguez ¹, Guadalupe Pena Contreras ², Haidar Ahmed ², Thadeu E. M. M. Costa ^{3,4} , Rachid Skouta ^{1,2,5,*} and Rosa A. Maldonado ^{1,*}

¹ Department of Biological Sciences, Border Biomedical Research Center, The University of Texas at El Paso, El Paso, TX 79968, USA; frodriguez16@miners.utep.edu (F.R.); eainiguez@miners.utep.edu (E.I.)

² Department of Chemistry, Border Biomedical Research Center, The University of Texas at El Paso, El Paso, TX 79968, USA; gpenacontreras@miners.utep.edu (G.P.C.); hahmed2@miners.utep.edu (H.A.)

³ Centro de Desenvolvimento Tecnológico em Saúde, Fundação Oswaldo Cruz, Rio de Janeiro, RJ 21040-361, Brazil; temmcosta@gmail.com

⁴ Instituto de Tecnologia em Fármacos-Farmanguinhos, Fundação Oswaldo Cruz, Rio de Janeiro, RJ 22775-903, Brazil

⁵ Department of Biology, University of Massachusetts, Amherst, MA 01003-9297, USA

* Correspondence: rskouta@umass.edu (R.S.); ramaldonado@utep.edu (R.A.M.); Tel.: +1-915-747-5318 (R.S.); +1-915-747-6891 (R.A.M.)

Received: 29 May 2018; Accepted: 3 July 2018; Published: 4 July 2018



Abstract: *Leishmania major* (*L. major*) is a protozoan parasite that causes cutaneous leishmaniasis. About 12 million people are currently infected with an annual incidence of 1.3 million cases. The purpose of this study was to synthesize a small library of novel thiophene derivatives, and evaluate its parasitic activity, and potential mechanism of action (MOA). We developed a structure–activity relationship (SAR) study of the thiophene molecule **5A**. Overall, eight thiophene derivatives of **5A** were synthesized and purified by silica gel column chromatography. Of these eight analogs, the molecule **5D** showed the highest in vitro activity against *Leishmania major* promastigotes (EC₅₀ 0.09 ± 0.02 μM), with an inhibition of the proliferation of intracellular amastigotes higher than 75% at only 0.63 μM and an excellent selective index. Moreover, the effect of **5D** on *L. major* promastigotes was associated with generation of reactive oxygen species (ROS), and in silico docking studies suggested that **5D** may play a role in inhibiting trypanothione reductase. In summary, the combined SAR study and the in vitro evaluation of **5A** derivatives allowed the identification of the novel molecule **5D**, which exhibited potent in vitro anti-leishmanial activity resulting in ROS production leading to cell death with no significant cytotoxicity towards mammalian cells.

Keywords: thiophene compounds; *Leishmania major*; cutaneous leishmaniasis; drug screening; chemotherapy; structure–activity relationship (SAR); in silico docking; reactive oxygen species

1. Introduction

Leishmaniasis is a devastating neglected tropical disease (NTD) [1] caused by the protozoan parasite of the genus *Leishmania*. The parasite is transmitted from animals to humans through the bite of infected females *Lutzomyia* or *Phlebotomus* sand flies [2]. Over 20 species and subspecies of *Leishmania* infect humans, causing three major clinical forms of the disease: cutaneous (CL), visceral, and mucocutaneous leishmaniasis [3]. The prevalence of CL, the most common form of leishmaniasis, is estimated between 0.7 and 1.3 million new annually cases worldwide [4], and it is commonly caused by *Leishmania major* (*L. major*) or *L. mexicana*. CL presents as singular ulcerative or nodular lesions at the

bite site that may resolve into scar tissue, often leading to scarring and social stigma [5]. The disease is present in both the Old World in regions of the Middle East, Africa, Central Western and Easter Europe; and the New World in regions of Central and South America, and more recently in North America [5].

Currently, there is no preventative or therapeutic human vaccine available against any clinical manifestation of the disease, and available treatments such as pentavalent antimonials (Glucantime and Pentostam), liposomal amphotericin B (AmBisome®), and miltefosine (IMPAVIDO®) present several disadvantages [6]. Pentavalent antimonial treatments are the first line of action, however, systemic therapy its required for more than 20 days, with toxic side effects including cardiotoxicity and hepatotoxicity [7,8]. Amphotericin B is highly active, but has extensive toxicity complications (nausea, vomiting, rigors, fever, hypertension or hypotension, and hypoxia) that usually lead to treatment interruption; besides, its administration requires hospitalization and its high cost limits its use in developed countries [5,9]. Miltefosine is the only oral agent against leishmaniasis, however, it presents several limitations such as embryo-fetal toxicity, fetal death, and its long half-life (150 h) may facilitate the emergence of drug resistance [10,11]. Thus, these facts clearly emphasize the urgent priority for the development of novel chemotherapies against leishmaniasis.

Considering the current interest in the search of antileishmanial agents, we previously reported for the first time that arylalkylamine type-compounds exhibit anti-*Leishmania* activity with no toxicity to mammalian cells [12,13]. Toward our medicinal chemistry effort in developing novel compounds with anti-parasitic activity and drug like properties (e.g., improved solubility, potency, stability and less or low toxicity), we assessed the antileishmanial activity of a series of novel compounds based on the thiophene scaffold with pharmaceutical properties: low toxicity, improved potency and solubility [13]. In this context, in the present study, we evaluated nine synthetic thiophene molecules derivatives against *L. major*.

We set a goal to design and synthesize a scaffold with antileishmanial activity in a one- or two-step synthesis using simple and efficient chemical transformations with high yield, high atom economy and inexpensive starting material. In this study, we focused on the creation of substituted thiophenes which are considered among the privileged structures in drug discovery [14]. Substituted thiophenes are known with their various biological activities such as anti-microbial, anti-cancer, and anti-inflammatory properties [14]. Therefore, the development of novel thiophene compounds with activity against *Leishmania* is crucial and urgent, as they may also complement current drugs and overcome drug resistance.

2. Results

2.1. Synthetic Chemistry

Toward synthesizing the substituted thiophene **5A** efficiently, we used the well establish three components coupling reaction between a ketone, cyanoacetate and elemental sulfur [15] followed by a simple acylation reaction. The synthesis of **5A** is depicted in Figure 1A. After synthesizing **5A**, we developed the Structure–Activity Relationship (SAR) of **5A** and created eight analogs, as shown in Figure 1B. The purity of each analog was confirmed by ¹H-NMR, ¹³C-NMR and MS, and then novel thiophene-like library compounds (Figure 2) were assessed for their potential in vitro antileishmanial activity.

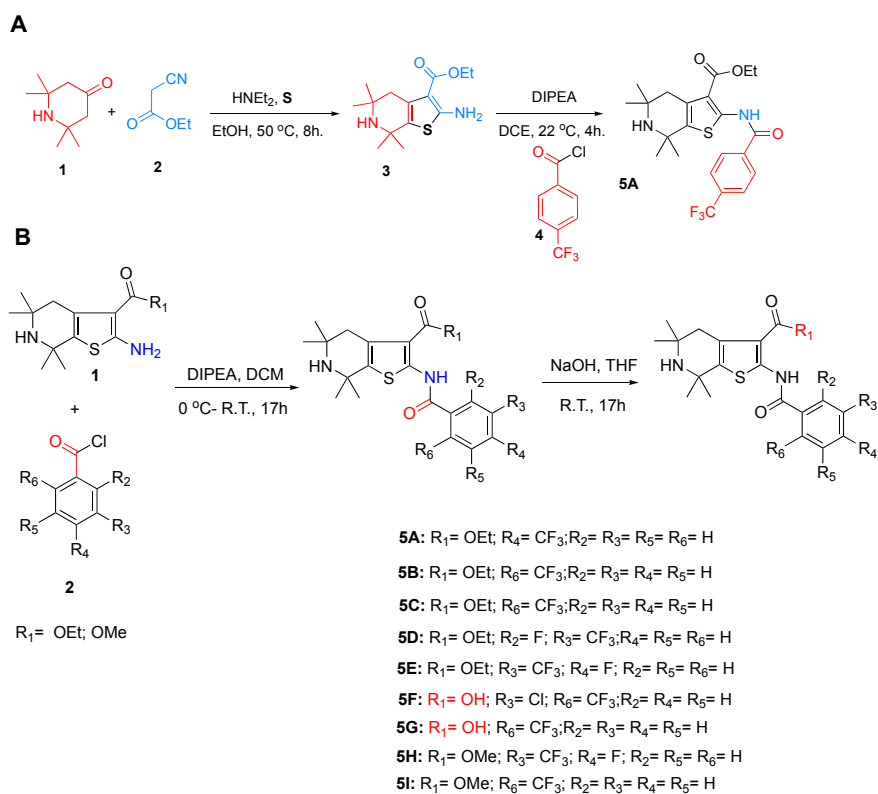


Figure 1. (A) Synthesis of thiophene **5A** (Ethyl 5,5,7,7-tetramethyl-2-(4-(trifluoromethyl)benzamido)-4,5,6,7-tetrahydrothieno [2,3-c]pyridine-3-carboxylate). (B) Synthetic route for the creation of thiophene compounds.

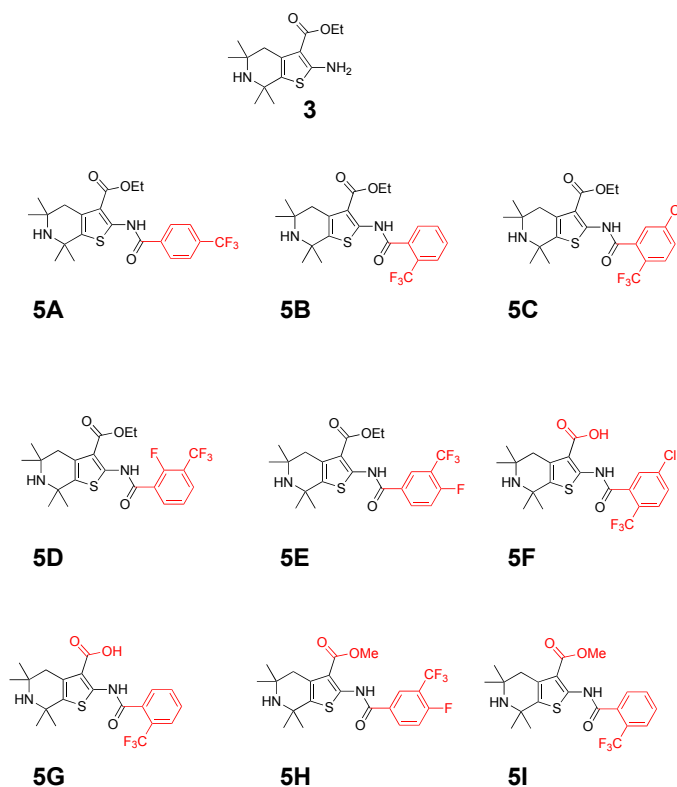


Figure 2. Chemical structures of the nine thiophene compounds.

2.2. Efficacy and Cytotoxicity of Parent Compound 5A

First, the efficacy of thiophene derivative **5A** was evaluated against transgenic *L. major* promastigotes expressing firefly luciferase (*L. major-luc*) as previously described [16,17]. Compound **5A** at a range of 0.31–10 μM was incubated with 2×10^6 *L. major-luc* promastigotes per mL for 72 h at 28 $^\circ\text{C}$, and in vitro parasite viability (% survival) was measured by luciferase activity. Compound **5A** displayed an approximate 50% effective concentration (EC_{50}) of 0.34 μM against *L. major* promastigotes (Figure 3 and Table 1). Furthermore, we investigated the potential cytotoxicity of **5A** by alamarBlue™ Cell Viability Assay (Thermo Fisher Scientific, Waltham, MA, USA) [18] and **5A** displayed a selective index (S.I.) of 30.58 against BALB/c intraperitoneal mouse macrophages (IP Φ), and 51.91 in monkey kidney cells (LLC-MK2) (Table 1).

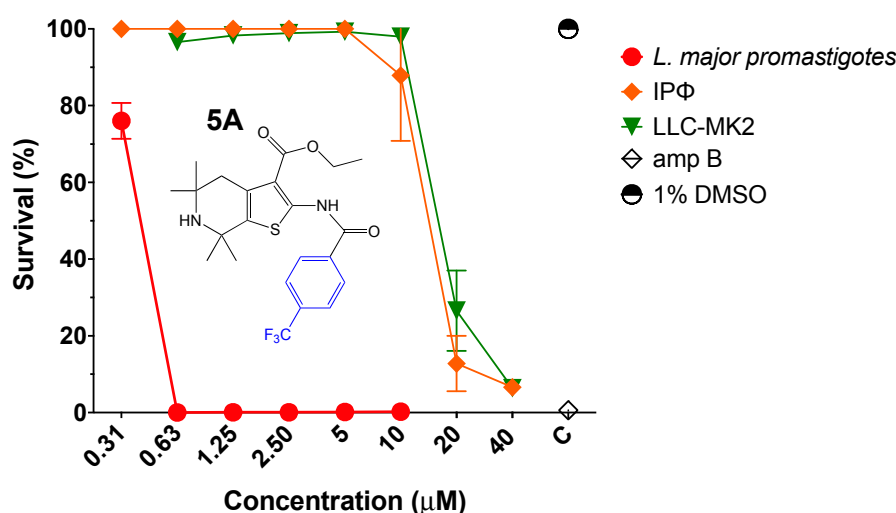


Figure 3. Antiparasitic effect of thiophene derivative **5A**. Viability of *L. major-luc* promastigotes incubated with **5A** at 0.31 to 10 μM for 72 h. Evaluation of intraperitoneal mouse macrophages (IP Φ) cytotoxicity for 48 h, or monkey kidney cells (LLC-MK2) treated with **5A** at concentrations of 0.31 to 40 μM for 72 h. Controls treated with 1% DMSO, or amphotericin B (amp B) at 5 μM .

Table 1. Antiparasitic activity in *L. major-luc* promastigotes, and cytotoxicity to intraperitoneal mouse macrophages (IP Φ) or monkey kidney cells (LLC-MK2) of **5A** and analogs. EC_{50} Median effective concentration. \pm values are the estimated EC_{50} interval. CC_{50} Median cytotoxic concentration. \pm values are the estimated CC_{50} interval S.I. Selective Index (CC_{50} mammalian cells)/(EC_{50} in *L. major-luc* promastigotes).

Compound	<i>Leishmania major-luc</i>		Mammalian Cells	
	Promastigotes		IP Φ	
	EC_{50} (μM)		CC_{50} (μM) [S.I.]	CC_{50} (μM) [S.I.]
5A	~0.3410		~10.40 [30.50]	17.69 \pm 1.12 [52.85]
5B	5.98 \pm 1.72		N/A	N/A
5C	4.73 \pm 0.69		N/A	N/A
5D	0.09 \pm 0.02		27.89 \pm 3.19 [310]	>80
5E	0.78 \pm 0.11		16.59 \pm 1.52 [21.27]	80 \pm 4.45 [102.56]
5F	>12.50		N/A	N/A
5G	>12.50		N/A	N/A
5H	3.05 \pm 0.47		N/A	N/A
5I	5.5 \pm 1.80		N/A	N/A

2.3. In Vitro Anti-Leishmanial Activity of Thiophene Derivatives and Their Cytotoxicity

Consequently, to lower the toxicity and increase the parasitic activity, eight new thiophene molecules (Figure 2) were evaluated. First, the thiophene compounds were tested in the presence of increasing drug concentrations (1.56–12.5 μM), followed by incubation with *L. major-luc* promastigotes ($2 \times 10^6/\text{mL}$) for 72 h at 28 °C. The experiment was performed using the same conditions as described for the parent drug 5A. As summarized in Table 1, all eight thiophene molecules showed promising antileishmanial activity against *L. major* promastigotes with an EC_{50} ranging from 0.09 to 6.25 μM (Figure 4A). However, the best thiophene compounds were 5D (EC_{50} 0.09 ± 0.02 μM) and 5E (EC_{50} 0.78 ± 0.11 μM) (Figure 4B and Table 1).

Consequently, cytotoxicity assays were performed by incubating LLC-MK2 or IP Φ with compounds. First, 5D or 5E were incubated with 1×10^5 LLC-MK2/mL or 1×10^5 IP Φ /mL for 72 and 48 h, respectively. Interestingly, compound 5D did not display perceptible toxicity against LLC-MK2 at concentrations up to 80 μM (Figure 4C,D). In the case of IP Φ , 5D exhibited a CC_{50} value of 27.89 ± 3.19 μM and an excellent S.I. of 310. As 5E compound CC_{50} values of 80 ± 4.45 μM in LLC-MK2 cells and 16.59 ± 1.52 μM in IP Φ , with S.I. values of 102.56 and 21.27, respectively. More importantly, we determined that both 5D and 5E displayed lower cytotoxicity to mammalian cells and higher parasitic activity than parent compound 5A (Table 1).

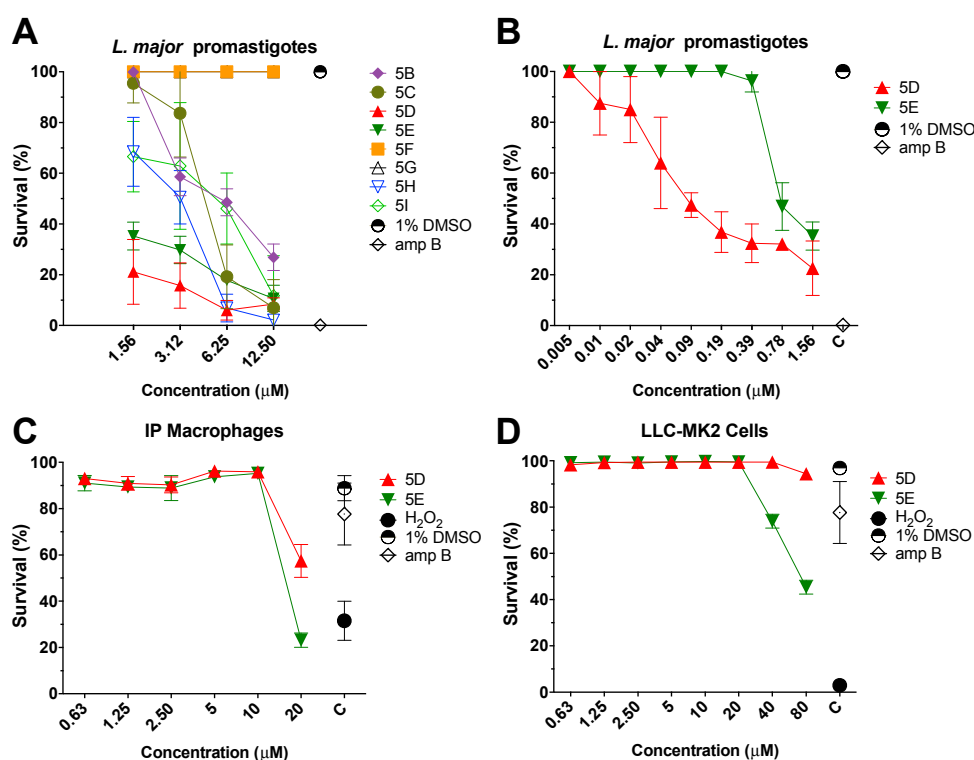


Figure 4. (A) Antiparasitic effect of the eight thiophene derivatives. Viability of *L. major-luc* promastigotes treated with the eight thiophene derivatives at a concentration of 1.56 to 12.5 μM for 72 h. (B) Evaluation of *L. major-luc* promastigotes treated with 5D or 5E thiophene derivatives at lower concentrations (0.005 to 1.56 μM) for 72 h. Controls treated with 1% DMSO, or amphotericin B (amp B) at 5 μM . (C) Cytotoxicity evaluation of intraperitoneal mouse macrophages (IP Φ) treated with 5D or 5E thiophene derivatives at concentrations from 0.63 to 20 μM for 48 h. (D) Cytotoxicity evaluation of monkey kidney cells (LLC-MK2) treated with 5D or 5E thiophene derivatives at a concentrations from 0.63 to 80 μM for 72 h. Controls treated with 1% DMSO, amp B at 5 μM , or 5% of hydrogen peroxide (H_2O_2). Cells were stained with Hoechst 33342 (healthy cell) and Propidium Iodide (compromised cell).

2.4. In Vitro Efficacy of Thiophene 5D Against Intracellular Amastigotes

Additionally, efficacy of thiophene compounds **5D** and **5E** was tested against the infectious intracellular amastigote form of *L. major*, by High-Content Imaging Assay (HCIA) on infected intraperitoneal mouse macrophages. As observed in Figure 5A, in comparison with untreated control and 1% DMSO, **5D** and **5E** inhibited the proliferation of the intracellular amastigotes by more than 75% and 50%, respectively, at a 0.625 μM concentration. Furthermore, as observed in Figure 5B, a reduced number of infected cells were observed after **5D** or **5E** treatment (2.5 μM) when compared to control treated with 1% DMSO.

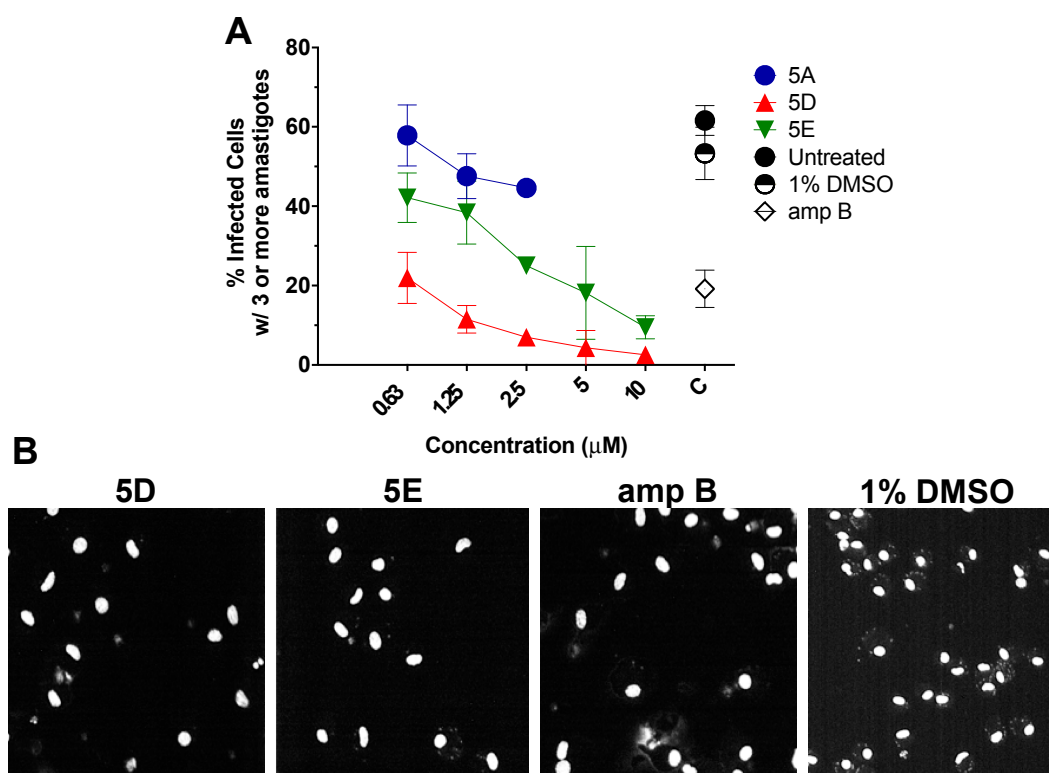


Figure 5. (A) High content imaging assay (HCIA) analysis of intraperitoneal mouse macrophages (IP Φ) infected with *L. major-luc* amastigotes, followed by treatment with **5D** or **5E** from 0.63 to 10 μM for 48 h. Controls included untreated, 1% DMSO, amphotericin B (amp B) at 5 μM , or parent drug **5A**. Data are represented as the percentage (%) of infected IP Φ with three or more amastigotes per cell. Note: Data for **5A** at concentration 5 and 10 μM were not generated because **5A** was cytotoxic for IP Φ at such concentration. (B) Representative monochromatic images of infected IP Φ with *L. major* after 48 h treatment with **5D** or **5E** at 2.5 μM , amp B (5 μM), or 1% DMSO.

2.5. Molecule 5D Induces ROS in *L. major*

Based on our previous study [12], it was hypothesized that **5D** may induce parasite death through the production of ROS. Thus, 2×10^6 *L. major* promastigotes per mL were incubated with **5D** (EC_{50} 0.09 ± 0.02 μM). After 24 h, ROS levels were measured by the addition of 10 μM of the cell-permeable dye H_2DCFDA (Thermo Fisher Scientific, Waltham, MA, USA), and fluorescence was monitored for an additional 7 h using a fluorometer. As expected, ROS levels in **5D** treated parasites were 14.5-fold higher compared to vehicle control 1% DMSO (Figure 6).

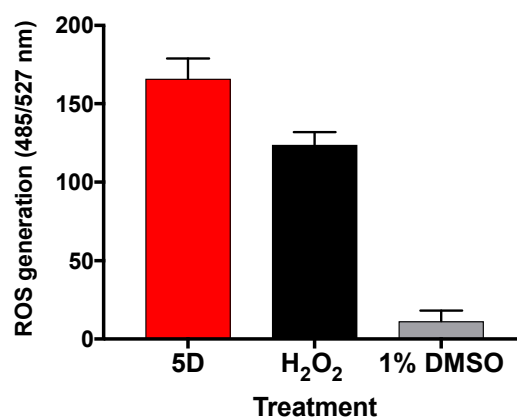
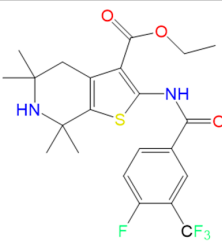
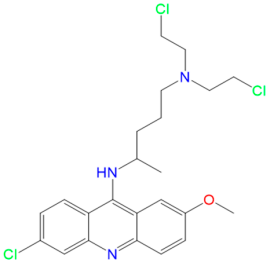


Figure 6. Generation of reactive oxygen species in *L. major* treated for 31 h with **5D** at 0.90 μM (EC_{50}). Values shown are the mean and standard error of five different replicates minus basal fluorescence. Control treated with 1% DMSO or hydrogen peroxide (H_2O_2) at 100 μM .

2.6. Docking of **5D** on TryR from *Leishmania*

Next, to determine the possible molecular mechanism responsible for the antileishmanial activity of **5D**, docking studies on TryR from *L. infantum* (PDB id: 2JK6) were performed. Using Glide Standard Precision [19] and Extra Precision (XP), we performed Rigid Receptor Docking analysis of control (Quinacrine Mustard) and **5D**. The 3D ligand structures were docked against the best potential binding site of 2JK6. Glide SP and XP only accounts for the ligand being dynamic however the protein remains rigid. Docking box coordinates and dimensions remained all at default ($20 \times 20 \times 20 \text{ \AA}$). Glide XP gives an output of a docking score, which was analyzed by the lowest number, or whichever is more negative to be the highest scoring ligand. The docking results, summarized in Table 2, showed the control (Quinacrine Mustard) with higher binding affinity than **5D** in both SP and XP. However, the XP docking score did not differ by much, indicating more rigorous docking analysis is needed. Thus, both ligands were taken to Schrodinger's Flexible receptor docking.

Table 2. In silico study of **5D** and control Quinacrine Mustard.

Receptor	Ligand	Structure	Glide SP (XP)	IFD XP (IFD Score)
TryR (2JK6)	5D		-4.6 (-5.5)	-10.0
	Quinacrine Mustard (control)		-6.9 (-6.7)	-9.2

Schrodinger IFD protocol for all IFD jobs was used [20]. The IFD program makes use of both Glide (for docking) and Prime (for protein structure modeling). The combination of the two software

packages allows a more accurate ligand binding calculation. We performed the re-docking with Glide XP for the refined docking results [21]. The IFD data presented in Table 2 show that our lead molecule **5D** had a better binding affinity. Docking scores from Rigid Receptor Docking and Flexible Receptor

Docking differed significantly. This is accounted for the protein dynamic movement during drug binding in IFD. Furthermore, Figure 7A,B presents the IFD binding pocket of the protein–ligand complex. Figure 7A shows our lead molecule **5D** which displays hydrogen bond interactions with SER 1632, ARG 287, VAL 55, and also with CYS 57. Compound **5D** also exhibits π -cation interaction with residue ARG 287. Quinacrine Mustard interacted with a new set of residues and showed only two hydrogen bonds between MET 333 and ALA 365 (Figure 7B). The control also formed salt bridges with ASP 327 as well as GLU 202. π - π and π -cation interaction was also shown between TYR 198 and LYS 60, respectively. These results provided evidence that the possible MOA of **5D** may be through the inhibition of TryR, an essential enzyme to the thiol metabolism of the parasite [22,23], and promising chemotherapeutic target against leishmaniasis [24].

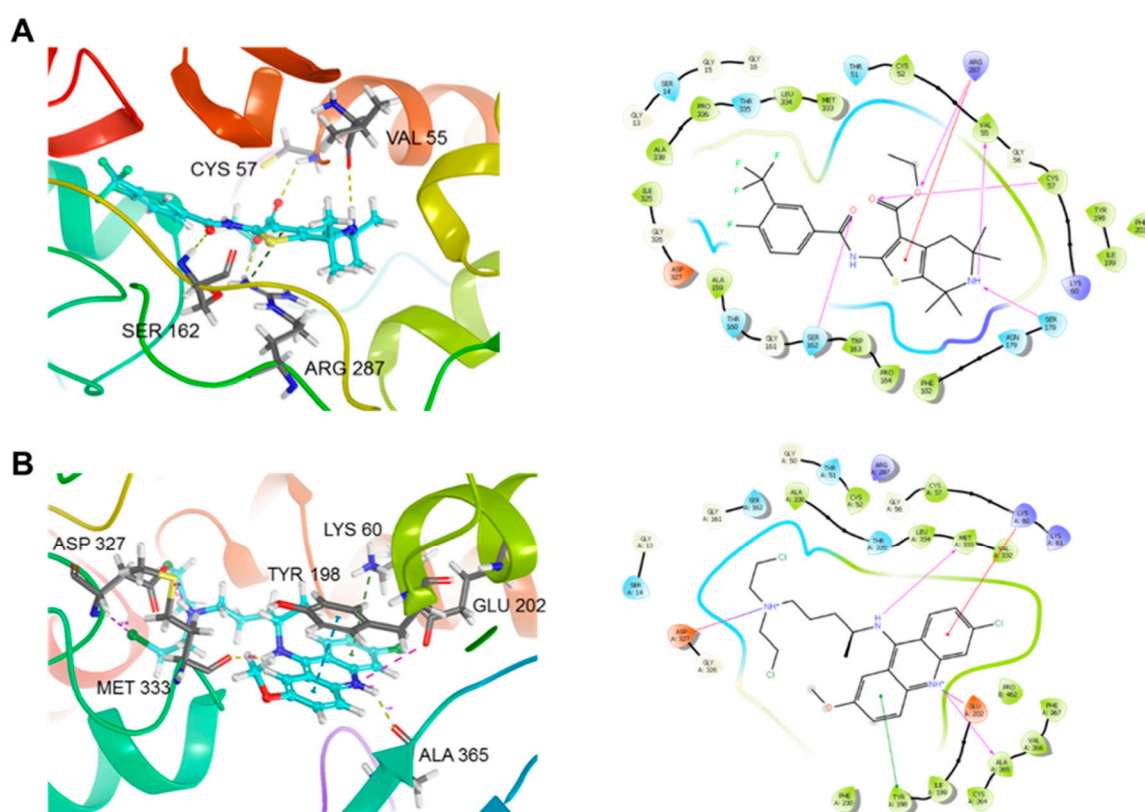


Figure 7. Trypanothione Reductase from *L. infantum* (PDB: 2JK6) Protein–ligand complex of Induced Fit Docking (IFD): (A) ligand interaction diagram of **5D** in complex with 2JK6 and 2D ligand interaction and; (B) ligand interaction diagram of Quinacrine Mustard in complex with 2JK6 and 2D ligand interaction.

3. Discussion

There is an urgent need for new therapeutics that are more effective and less toxic than conventional treatments used to treat infectious diseases, including leishmaniasis [25]. Thiophenes derivatives are known for their therapeutic applications and have shown promising results to treat different types of cancer, degenerative diseases, HIV, and malaria [26–33]. Thus, we evaluated the anti-leishmania activity and selectivity of nine thiophene derivatives against *L. major*, and potential MOA was elucidated for our best candidate, **5D**.

Thiophene derivatives **5A**, **5D** and **5E** exhibited potent parasitic activity against *L. major* promastigotes (Table 1). Experimental models involving macrophages are ideal to study leishmaniasis since they are the major host cell for *Leishmania* spp. [34]. Thus, our three best candidates were further evaluated against the most important form of the parasite, intracellular amastigotes, in an in vitro infection model of murine macrophages. In this case, **5D** presented the best anti-leishmanial activity by decreasing the proliferation of the parasite by 80%.

The in vitro toxicity of **5D** and **5E** was evaluated towards IP Φ and LCC-MK2 cells. Our best two compounds were safer for the two cytotoxic models than the reference drug, amphotericin B, which is already known for its cytotoxic effects [35]. Even though amphotericin B presented similar activity as **5D** against promastigotes and amastigotes, this result further supports the application of **5D** and **5E** as anti-leishmanial agents. Furthermore, the selectivity presented by **5D** was remarkably higher than the parent compound **5A** (10-fold higher), demonstrating the success to increase the anti-leishmanial activity and reduced cytotoxicity effects when compared to our previously reported arylalkylamine type-compound [12].

Next, we studied the potential MOA of derivative **5D**. ROS can be generated in response to some drugs, resulting in destruction of cellular macromolecular components inducing cell death by affecting parasite mitochondrial function [36,37]. Here, we observed that **5D** induced ROS production in *L. major* promastigotes after 31 h of treatment. The redox homeostasis in *Leishmania* is achieved through the activity of several superoxide dismutases, heme peroxidases, as well as of a series of thiol-containing proteins that directly or indirectly depend on trypanothione reductase [23,38]. In this regard, the trypanothione metabolism is unique to trypanosomatids and its main detoxification pathway [39]. This pathway protects parasites from oxidative stress and participates in several cellular processes that are carried out by glutathione in other organisms. Moreover, there are several trypanothione-dependent pathways that include enzymes such as tryparedoxin peroxidase (detoxication of hydroperoxide), ascorbate peroxidase (homeostasis of ascorbate), ribonucleotide reductase (synthesis of DNA precursors), and others [40,41]. With this idea on mind, we decided to explore in silico docking analysis to assess the possibility of *L. major* TryR as the target of **5D**. Moreover, our results suggested that TryR interacts with **5D**, however we do not exclude the possibility that other redox metabolism enzymes could be also targeted by compound.

In conclusion, to discover new chemotherapy agents against leishmaniasis, we efficiently synthesized nine thiophene type-compounds including **5A**, following a two-step synthesis from low-priced commercially available starting materials. We then showed that our novel thiophene type-compounds possess high in vitro antileishmanial activity. Based on our SAR study, **5D** analog was selected as the most promising lead compound among this library with excellent antiparasitic and S.I. Furthermore, **5D** may act against trypanothione metabolism, followed by the production of ROS in the parasite; nevertheless, biological studies with recombinant TryR enzyme needs to be performed to further support this assumption. Overall, **5D** represents a potential chemotherapeutic agent for the treatment of leishmaniasis, and further evaluation in a pre-clinical mouse model of cutaneous leishmaniasis is currently in progress in our laboratory.

4. Materials and Methods

4.1. General

Unless otherwise noted, all commercial reagents were used as purchased from Aldrich, St. Louis, MO, USA. All the reactions were monitored by thin-layer chromatography (TLC) that was performed on silica gel plates GF254. Compounds were visualized under a UV lamp. Flash chromatography was performed using silica gel (200–300 mesh) with various ratios of Dichloromethane: Methanol solvents as indicated in the text. Spectroscopy: ^1H and ^{13}C -NMR spectra were obtained on a Bruker DPX 400 MHz. Chemical shifts (δ) are quoted in parts per million (ppm), to the nearest 0.01 ppm and internally referenced relative to the solvent nuclei. ^1H -NMR spectral data are reported with their

chemical shift in parts per million (ppm). The multiplicity in $^1\text{H-NMR}$ is abbreviated as follows: brs: broad; s: singlet; d: doublet; t: triplet; q: quartet; quint: quintet; sext: sextet; *m*: multiplet; or as a combination (e.g., dd, dt, etc.). The coupling constant (*J*) in hertz, integration and proton count were determined.

Spectrometer: Liquid chromatography/mass spectra (LC-MS) [+ESI] were taken on double focusing sector type mass spectrometer HX-110A. Maker JEOL Ltd. Tokyo, Japan (resolution of 10,000 and 10 KV accel. Volt. Ionization method; FAB (Fast Atom Bombardment) used Xe 3 KV energy. Used Matrix, NBA (m-Nitro benzyl alcohol)). Melting points were measured using a Mel-Temp melting point apparatus.

4.2. Chemical Synthesis

4.2.1. General Synthetic Procedure 1

Synthesis of the Ethyl 5,5,7,7-tetramethyl-2-(4-(trifluoromethyl) benzamido)-4,5,6,7-tetrahydrothieno [2,3-c]pyridine-3-carboxylate (5A)

Briefly, the 2,2,6,6-tetramethylpiperidine ketone (**1**, 1 equivalent) was mixed with 2-cyanoacetate esters (**2**, 1 equivalent) and elemental sulfur (1 equivalent) in the presence of diethylamine (3 equivalents) in ethanol (EtOH) at 60 °C for 17 h. The crude was precipitated by adding water and filtered to provide the desired known 2-aminothiophene intermediate (**3**) [12]. The latter was reacted with 4-trifluoromethyl benzoyl chloride in the presence of diisopropylethylamine in dry dichloromethane at 0 °C for 1 h and then at room temperature for 4 h. The solvent was evaporated then the crude mixture was purified by flash-column chromatography on silica gel, using a mixture of solvent of dichloromethane: methanol (DCM: MeOH) at ratios from 100:1 to 50:1, to provide the desired ethyl 5,5,7,7-tetramethyl-2-(4-(trifluoromethyl)benzamido)-4,5,6,7-tetrahydrothieno [2,3-c]pyridine-3-carboxylate (**5A**) as a light brown solid. The purity of **5A** was confirmed by $^1\text{H-NMR}$, $^{13}\text{C-NMR}$, LC/MS and melting point.

4.2.2. General Synthetic Procedure 2

Synthesis of 5,5,7,7-tetramethyl-2-(2-(trifluoromethyl)benzamido)-4,5,6,7-tetrahydrothieno [2,3-c]pyridine-3-carboxylic acid (5G)

To ethyl 5,5,7,7-tetramethyl-2-(2-(trifluoromethyl)benzamido)-4,5,6,7-tetrahydrothieno [2,3-c]pyridine-3-carboxylate compound (**5B**; 1 equiv.) in 1 mL of tetrahydrofuran (THF), was added 5 equiv. of sodium hydroxide (NaOH) in water (1 mL). The mixture was stirred at room temperature during 17 h. The THF solvent was evaporated then mixture was acidified with HCl 1M to pH = 4. The protonated acid compound was extracted with ethylacetate (EtOAc) (3×; 50 mL) then dried under magnesium sulfate (MgSO_4), and the solvent was evaporated to provide the desired 5,5,7,7-tetramethyl-2-(2-(trifluoromethyl)benzamido)-4,5,6,7-tetrahydrothieno [2,3-c]pyridine-3-carboxylic acid (**5G**), (Figure 2). The purity of **5G** analog was confirmed by $^1\text{H-NMR}$, $^{13}\text{C-NMR}$, and LC/MS.

Following the general synthetic procedure 1, and in the presence of various substituted benzoyl chlorides, we created the analogs **5B–5E**, and **5H–5I**.

Ethyl-5,5,7,7-tetramethyl-2-(2-(trifluoromethyl)benzamido)-4,5,6,7-tetrahydrothieno[2,3-c]pyridine-3-carboxylate (5B)

Brown solid, yield 75%, m.p. 181.5–182.5 °C. $^1\text{H-NMR}$ (400 MHz, CDCl_3) δ 11.68 (s, 1H, NHCO), 7.78–7.65 (m, 4H, ArH), 4.32 (q, *J* = 7.0 Hz, 3H, CH_2), 2.70 (s, 2H, CH_2), 1.92 (m, 1H, NH), 1.39–1.16 (m, 15H, 5 × CH_3). $^{13}\text{C-NMR}$ (101 MHz, CDCl_3) δ 166.18, 163.70, 147.33, 135.09, 133.90, 132.18, 130.71, 128.50, 128.32, 126.68, 112.30, 60.61, 51.89, 49.84, 39.53, 34.13, 29.99, 14.00. LC-MS (ESI) for $\text{C}_{22}\text{H}_{25}\text{F}_3\text{N}_2\text{O}_3\text{S}$, $M + 1 = 455.22$.

Ethyl-5,5,7,7-tetramethyl-2-(2-(trifluoromethyl)benzamido)-4,5,6,7-tetrahydrothieno[2,3-c]pyridine-3-carboxylate (5C)

Brown solid, yield 70%, m.p. 132.6–133.6 °C. ¹H-NMR (400 MHz, CDCl₃) δ 11.56 (s, 1H, NHCO), 7.52–7.40 (m, 3H, ArH), 4.10 (q, *J* = 7.1 Hz, 3H, CH₂), 2.53 (s, 2H, CH₂), 1.32–1.03 (s, 15H, 5 × CH₃). ¹³C-NMR (101 MHz, CDCl₃) δ 166.05, 162.14, 146.93, 138.40, 135.50, 135.04, 130.73, 128.58, 128.43, 128.25, 126.30, 112.53, 60.69, 52.17, 50.17, 39.27, 33.88, 29.71, 13.96. (ESI+, *M* + 1 = 489.02. LC-MS (ESI) for C₂₂H₂₄ClF₃N₂O₃S, *M* + 1 = 489.02.

Ethyl-2-(2-fluoro-3-(trifluoromethyl)benzamido)-5,5,7,7-tetramethyl-4,5,6,7-tetrahydrothieno[2,3-c]-pyridine-3-carboxylate (5D)

Light brown solid, yield 76%, m.p. 145.4–146.4 °C. ¹H-NMR (400 MHz, CDCl₃) δ 12.40 (d, *J* = 10.3 Hz, 1H, NHCO), 8.49–8.30 (m, 1H, ArH), 7.83 (dd, *J* = 10.5, 3.9 Hz, 1H, ArH), 7.45 (t, *J* = 7.8 Hz, 1H, ArH), 4.42 (q, *J* = 7.1 Hz, 2H, CH₂), 2.74 (s, 2H, CH₂), 1.54 (s, 6H, 2 × CH₃), 1.42 (t, *J* = 7.1 Hz, 3H, CH₃), 1.23 (t, *J* = 7.1 Hz, 6H, 2 × CH₃). ¹³C-NMR (101 MHz, CDCl₃) δ 165.70, 158.50, 146.67, 136.26, 135.74, 131.23, 129.15, 124.87, 123.48, 121.53, 119.30, 113.11, 60.86, 52.03, 50.01, 39.71, 34.34, 30.23, 14.29. LC-MS (ESI) for C₂₂H₂₄F₄N₂O₃S, *M* + 1 = 473.05.

Ethyl-2-(4-fluoro-3-(trifluoromethyl)benzamido)-5,5,7,7-tetramethyl-4,5,6,7-tetrahydrothieno[2,3-c]-pyridine-3-carboxylate (5E)

Light brown solid, yield 66%, m.p. 116.0–117.0 °C. ¹H-NMR (400 MHz, CDCl₃) δ 12.40 (s, 1H, NHCO), 8.25 (dd, *J* = 6.4, 1.4 Hz, 1H, ArH), 8.10 (ddd, *J* = 7.9, 4.1, 2.2 Hz, 1H, ArH), 7.29 (t, *J* = 9.1 Hz, 1H, ArH), 4.34 (q, *J* = 7.1 Hz, 2H, CH₂), 2.65 (s, 2H, CH₂), 1.46 (s, 6H, 2 × CH₃), 1.36 (t, *J* = 7.1 Hz, 3H, CH₃), 1.16 (d, *J* = 11.3 Hz, 6H, 2 × CH₃). ¹³C-NMR (101 MHz, CDCl₃) δ 166.89, 160.81, 148.04, 135.17, 132.73, 128.95, 128.58, 127.43, 119.35, 117.73, 117.51, 112.28, 60.92, 53.37, 52.12, 50.08, 39.57, 34.13, 30.03, 14.18. LC-MS (ESI) for C₂₂H₂₄F₄N₂O₃S, *M* + 1 = 473.05.

Methyl-2-(4-fluoro-3-(trifluoromethyl)benzamido)-5,5,7,7-tetramethyl-4,5,6,7-tetrahydrothieno[2,3-c]-pyridine-3-carboxylate (5H)

Light brown solid, yield 72%, m.p. 122.0–123.0 °C. ¹H-NMR (400 MHz, CDCl₃) δ 12.45 (s, 1H, NHCO), 8.32 (s, 1H, ArH), 8.18 (s, 1H, ArH), 7.37 (t, *J* = 8.0 Hz, 1H, ArH), 3.93 (s, 3H, CH₃), 2.71 (s, 2H, CH₂), 1.53 (s, 6H, 2 × CH₃), 1.27–1.16 (m, 9H, 3 × CH₃). ¹³C-NMR (101 MHz, CDCl₃) δ 167.47, 161.06, 160.86, 148.44, 132.84, 132.74, 129.03, 128.46, 127.53, 117.86, 117.64, 112.17, 52.45, 51.80, 50.45, 39.49, 34.13, 29.98. LC-MS (ESI) for C₂₁H₂₂F₄N₂O₃S, *M* + 1 = 459.07.

Methyl-5,5,7,7-tetramethyl-2-(2-(trifluoromethyl)benzamido)-4,5,6,7-tetrahydrothieno[2,3-c]pyridine-3-carboxylate (5I)

Light brown solid, yield 60%, m.p. 184.2–185.2 °C. ¹H-NMR (400 MHz, CDCl₃) δ 11.67 (s, 1H, NHCO), 7.78 (d, *J* = 7.4 Hz, 1H, ArH), 7.66 (dd, *J* = 10.9, 4.5 Hz, 3H, ArH), 3.85 (s, 3H, CH₃), 2.68 (s, 2H, CH₂), 1.52 (s, 6H, 2 × CH₃), 1.23 (s, 6H, 2 × CH₃). ¹³C-NMR (101 MHz, CDCl₃) δ 166.90, 164.03, 147.80, 135.24, 134.04, 132.27, 130.83, 128.57, 127.92, 126.90, 126.85, 112.18, 52.18, 51.64, 50.17, 39.59, 34.26, 30.12. LC-MS (ESI) for C₂₁H₂₃F₃N₂O₃S, *M* + 1 = 441.07.

Following the general synthetic procedure 2, we created the analogs 5F and 5G.

2-(5-chloro-2-(trifluoromethyl)benzamido)-5,5,7,7-tetramethyl-4,5,6,7-tetrahydrothieno[2,3-c]pyridine-3-carboxylic acid (5F)

Brown oilsh, yield 51% ¹H-NMR (400 MHz, CDCl₃) δ 11.69 (s, 1H, NHCO), 7.57–7.44 (m, 3H, ArH), 2.53 (s, 2H, CH₂), 1.32–1.03 (s, 12H, 4 × CH₃). ¹³C-NMR (101 MHz, CDCl₃) δ 167.09, 164.14, 161.83, 139.04, 135.50, 135.04, 130.73, 128.58, 128.43, 128.25, 126.30, 112.53, 52.17, 50.17, 39.27, 33.88, 29.71. LC-MS (ESI) for C₂₂H₂₄ClF₃N₂O₃S, *M* + 1 = 461.03.

5,5,7,7-tetramethyl-2-(2-(trifluoromethyl)benzamido)-4,5,6,7-tetrahydrothieno[2,3-c]pyridine-3-carboxylic acid (5G)

Brown oily, yield 55%. $^1\text{H-NMR}$ (400 MHz, CDCl_3) δ 11.70 (s, 1H, NHCO), 7.92–7.62 (m, 4H, ArH), 2.70 (s, 2H, CH_2), 1.39–1.16 (m, 12H, $4 \times \text{CH}_3$). $^{13}\text{C-NMR}$ (101 MHz, CDCl_3) δ 167.08, 163.70, 162.03, 136.09, 134.01, 132.18, 130.71, 128.50, 128.32, 126.68, 112.30, 51.89, 49.84, 39.53, 34.13, 29.99. LC-MS (ESI) for $\text{C}_{22}\text{H}_{25}\text{F}_3\text{N}_2\text{O}_3\text{S}$, $M + 1 = 427.02$.

4.3. Cell Maintenance

Transgenic *L. major* promastigotes expressing firefly luciferase (*L. major-luc*) (Lmj-FV1-LUC-TK [*L. major* strain Friedlin (MHOM/JL/80/Friedlin)]) were maintained in M199 medium supplemented with hemin, 10% inactivated fetal bovine serum (iFBS) (Gibco, Thermo Fisher Scientific, Waltham, MA, USA), and 1% of 10,000 units/mL penicillin and 10 mg/mL streptomycin (Gibco, Thermo Fisher Scientific, Waltham, MA, USA) as described [42]. Intraperitoneal murine macrophages (IP Φ) were obtained from BALB/c mice [43]. Monkey kidney epithelial cells (LLC-MK2) (ATCC # CCL-7) (American Type Culture Collection, Manassas, VA, USA), and IP Φ were cultured in Dulbecco's Modified Eagle's Medium (DMEM), supplemented with 10% iFBS, along with 1% of 10,000 units/mL penicillin and 10 mg/mL streptomycin. The procedures were performed minimizing the distress and pain for animals following the NIH guidance and animal protocol (A-201107-1) approved by UTEP's Institutional Animal Care and Use Committee (IACUC).

4.4. Luciferase Assay—Viability of *Leishmania Major* promastigotes

The antiparasitic activity of the 9 thiophene compounds was determined by adding the analogs together with 2×10^6 *L. major-luc* promastigotes per mL in 96-well NUNC white microplates (Thermo Fisher Scientific, Waltham, MA, USA) followed by incubation for 72 h at 28 °C. Then, parasite survival was measured by luciferase activity with the addition of the substrate 5'-fluoroluciferin (ONE-Glo luciferase assay system; Promega, Madison, WI, USA), using a luminometer (Luminoskan; Thermo Fisher Scientific, Waltham, MA, USA). The luminescence intensity was a direct measure of the parasite survival, and 50% effective concentration (EC_{50}) was determined for each drug and summarized in Table 1.

4.5. Assessment of Thiophene Compound Mammalian Cell Cytotoxicity

The potential cytotoxicity of 5A was tested by alamarBlueTM Cell Viability Assay (Thermo Fisher Scientific, Waltham, MA, USA) as previously described [18]. Briefly, 1×10^6 /mL rhesus monkey kidney epithelial cells (LLC-MK2), and 1×10^6 /mL BALB/c IP Φ were seeded in a 96-well clear bottom black microplate (BD Biosciences, Franklin Lakes, NJ, USA). Cells were incubated in the presence of increasing drug concentrations for 72 h (LLC-MK2) or 48 h (IP Φ) at 37 °C, 5% CO_2 , followed by addition of alamarBlueTM. Fluorescence was measured using a fluorometer (Fluoroskan; Thermo Fisher Scientific, Waltham, MA, USA). Compound 5D or 5E were incubated with 1×10^5 cells/mL (LLC-MK and IP Φ) for 72 or 48 h, respectively, at 37 °C, 5% CO_2 . After the incubation period, a dilution of 20:1000 in PBS from a stock at 1 mg/mL of Propidium Iodide (PI) and Hoechst 33342 (Thermo Scientific, Waltham, MA, USA) were added for survival discrimination as previously described [44]. Analysis was performed by High-Content Imaging Assay (HCIA) using an IN Cell 2000 Analyzer Bioimaging System (GE Healthcare, Chicago, IL, USA) for LLC-MK2 cells, and BD Pathway 855 High-resolution Bioimager System (BD Biosciences, Franklin Lakes, NJ, USA) for IP Φ . The 50% cytotoxic concentration (CC_{50}) and selective index (S.I.) was determined and summarized in Table 1.

4.6. High-Content Imaging Assay—Proliferation Experiments

BALB/c IP Φ were acquired and seeded at a density of 1×10^5 cells/mL for 2 h at 37 °C, 5% CO_2 . After adherence, IP Φ were infected with 1×10^6 /mL metacyclic promastigotes of *L. major-luc*, at a ratio

of 10:1 parasites per macrophage. Subsequently, infected IP Φ were incubated with derivatives **5A**, **5D** and **5E** at increasing concentrations (0.625 to 10 μ M) for 48 h treatment. Afterwards, cells were fixed with 4% paraformaldehyde, and stained with (1.25:100) Alexa Fluor™ 488 Phalloidin (Thermo Fisher Scientific, Waltham, MA, USA) and (1:1000) DAPI (Sigma Aldrich, St. Louis, MO, USA). Then, the numbers of infected cells and amastigotes were determined by HCIA using an IN Cell 2000 Analyzer Bioimaging System (GE Healthcare, Chicago, IL, USA). Parameters were set for the excitation and emission spectra of Alexa Fluor™ 488 Phalloidin and DAPI, and a constraint of 3 or more parasites per macrophage was set as previously reported [44,45].

4.7. Measurement of Reactive Oxygen Species Levels

L. major promastigotes (2×10^6 cells/mL) were incubated for 24 h with **5D** (EC₅₀ 0.90 μ M) in a 96-well clear bottom black microplate (BD Biosciences, Franklin Lakes, NJ, USA). Controls treated with 1% DMSO, 100 μ M of hydrogen peroxide (H₂O₂) as positive control, or M199 medium. After incubation period, 10 μ M of H₂DCFDA (Thermo Fisher Scientific, Waltham, MA, USA) (H₂DCFDA/DMSO, 1 mg/mL) was added per well followed by 20 min of incubation at 37 °C. Fluorescence was measured for an additional 7 h using a fluorometer (Fluoroskan; Thermo Fisher Scientific, Waltham, MA, USA) at 527 nm using an excitation wavelength of 485. For all measurements, basal fluorescence was subtracted.

All graphs, EC₅₀ and CC₅₀ values were produced using Graph Pad Prism 7 Software (GraphPad Software, Inc., La Jolla, CA, USA).

4.8. Docking Studies—Pre-Docking Preparation

The structure of trypanothione reductase bound to Flavin adenine dinucleotide (PDB ID: 2JK6) [46] were obtained from the Protein Data Bank. The Protein Preparation Wizard in Maestro was used to minimize the protein structure, add hydrogens and charges, and find any missing residues. The two-dimensional structures of **5D** and Quinacrine Mustard, a recently experimentally approved drug as a control, were drawn using the molecular structure editor ChemDraw Software (PerkinElmer, Waltham, MA, USA) and processed by LigPrep Schrödinger (Schrödinger, LLC., New York, NY, USA) to generate the 3D structures.

4.9. Binding Site Analysis

Maestro's SiteMap tool (Schrödinger, LLC., New York, NY, USA) was used to predict the likely binding sites of trypanothione reductase. The SiteMap tool uses a series of algorithm that generates a map of hydrophobic and hydrophilic surfaces on the protein surface [47]. Hydrophilic surface maps are divided into donor, acceptor, and metal-binding regions. Five potential binding sites were identified with at least 15 site points. However, the top SiteMap was chosen to be the receptor grid.

Author Contributions: Conceptualization, E.I., R.S. and R.A.M.; Methodology, E.I., R.S. and R.A.M.; Software, H.A.; Validation, F.R., E.I., G.P.C., H.A., R.S. and R.A.M.; Formal Analysis, F.R., E.I., G.P.C., H.A., T.E.M.M.C., R.S. and R.A.M.; Investigation, F.R., E.I., G.P.C., H.A. and T.E.M.M.C.; Resources, R.S. and R.A.M.; Data Curation, F.R., E.I., R.S. and R.A.M.; Writing—Original Draft Preparation, F.R., E.I., R.S. and R.A.M.; Writing—Review and Editing, F.R., E.I., R.S. and R.A.M.; Visualization, F.R., E.I., H.A., R.S. and R.A.M.; Supervision, R.S. and R.A.M.; Project Administration, R.S. and R.A.M.; and Funding Acquisition, R.S. and R.A.M.

Funding: This research was funded by: UTEP/BBRC Core Facilities: Biomolecule Analysis (BACF), Cytometry, Screening and Imaging (CSI), and Genomic Analysis (GACF) supported by NIGMS grant No. 5G12MD007592. The synthesis and docking sections were performed by Rachid Skouta research laboratory partially supported by the Lung Cancer Research Foundation and the Green Fund. E.I. was supported by the RISE Scholars Program at UTEP through grant No. R25GM069621-11 from the NIGMS. G.P.C. was supported by The UT System Louis Stokes Alliance for Minority Participation (LSAMP) funded by the National Science Foundation (grant number HRD-1202008). TEMMC was supported by the National Institutes of Science and Technology (INCT-IDN, Brazil) Science without Borders Program/CNPq.

Conflicts of Interest: The authors declare no conflict of interest.

References

1. Alvar, J.; Velez, I.D.; Bern, C.; Herrero, M.; Desjeux, P.; Cano, J.; Jannin, J.; den Boer, M.; WHO Leishmaniasis Control Team. Leishmaniasis worldwide and global estimates of its incidence. *PLoS ONE* **2012**, *7*, e35671. [[CrossRef](#)] [[PubMed](#)]
2. Aoun, K.; Bouratbine, A. Cutaneous leishmaniasis in North Africa: A review. *Parasite* **2014**, *21*, 14. [[CrossRef](#)] [[PubMed](#)]
3. Cappai, R.; Morris, L.; Aebischer, T.; Bacic, A.; Curtis, J.M.; Kelleher, M.; McLeod, K.S.; Moody, S.F.; Osborn, A.H.; Handman, E. Ricin-resistant mutants of *Leishmania major* which express modified lipophosphoglycan remain infective for mice. *Parasitology* **1994**, *108*, 397–405. [[CrossRef](#)] [[PubMed](#)]
4. World Health Organization. Leishmaniasis-Fact Sheet N°375. 2014. Available online: <http://www.who.int/mediacentre/factsheets/fs375/en/> (accessed on 9 May 2016).
5. McGwire, B.S.; Satoskar, A.R. Leishmaniasis: Clinical syndromes and treatment. *QJM* **2014**, *107*, 7–14. [[CrossRef](#)] [[PubMed](#)]
6. Rodrigues, K.A.; Dias, C.N.; Néris, P.L.; Rocha Jda, C.; Scotti, M.T.; Scotti, L.; Mascarenhas, S.R.; Veras, R.C.; de Medeiros, I.A.; Keesen Tde, S.; et al. 2-Amino-thiophene derivatives present antileishmanial activity mediated by apoptosis and immunomodulation in vitro. *Eur. J. Med. Chem.* **2015**, *106*, 1–14. [[CrossRef](#)] [[PubMed](#)]
7. Croft, S.L.; Coombs, G.H. Leishmaniasis—current chemotherapy and recent advances in the search for novel drugs. *Trends Parasitol.* **2003**, *19*, 502–508. [[CrossRef](#)] [[PubMed](#)]
8. Kato, K.C.; Morais-Teixeira, E.; Reis, P.G.; Silva-Barcellos, N.M.; Salaun, P.; Campos, P.P.; Dias Correa-Junior, J.; Rabello, A.; Demicheli, C.; Frezard, F. Hepatotoxicity of pentavalent antimonial drug: Possible role of residual Sb(III) and protective effect of ascorbic acid. *Antimicrob. Agents Chemother.* **2014**, *58*, 481–488. [[CrossRef](#)] [[PubMed](#)]
9. Laniado-Laborin, R.; Cabrales-Vargas, M.N. Amphotericin B: Side effects and toxicity. *Rev. Iberoam. Micol.* **2009**, *26*, 223–227. [[CrossRef](#)] [[PubMed](#)]
10. Nagle, A.S.; Khare, S.; Kumar, A.B.; Supek, F.; Buchynskyy, A.; Mathison, C.J.N.; Chennamaneni, N.K.; Pendem, N.; Buckner, F.S.; Gelb, M.H.; et al. Recent developments in drug discovery for leishmaniasis and human African trypanosomiasis. *Chem. Rev.* **2014**, *114*, 11305–11347. [[CrossRef](#)] [[PubMed](#)]
11. Turner, K.G.; Vacchina, P.; Robles-Murguía, M.; Wadsworth, M.; McDowell, M.A.; Morales, M.A. Fitness and Phenotypic Characterization of Miltefosine-Resistant *Leishmania major*. *PLoS Negl. Trop. Dis.* **2015**, *9*, e0003948. [[CrossRef](#)] [[PubMed](#)]
12. Iniguez, E.A.; Perez, A.; Maldonado, R.A.; Skouta, R. Novel arylalkylamine compounds exhibits potent selective antiparasitic activity against *Leishmania major*. *Bioorg. Med. Chem. Lett.* **2015**, *25*, 5315–5320. [[CrossRef](#)] [[PubMed](#)]
13. Skouta, R.M.R.A. Preparation of Tetramethyltetrahydrothienopyridine Derivatives for Use as Parasiticides. U.S. Patent Appl. Publ 20160362420 A1, 15 December 2016.
14. Keri, R.S.; Chand, K.; Budagumpi, S.; Balappa Somappa, S.; Patil, S.A.; Nagaraja, B.M. An overview of benzo[b]thiophene-based medicinal chemistry. *Eur. J. Med. Chem.* **2017**, *138*, 1002–1033. [[CrossRef](#)] [[PubMed](#)]
15. Sensfuss, U.; Habicher, W.D. 2-aminothiophenes from triacetoneamine: A convenient way to novel sterically hindered piperidine derivatives. *Heteroat. Chem.* **1998**, *9*, 529–536. [[CrossRef](#)]
16. Thalhofer, C.J.; Graff, J.W.; Love-Homan, L.; Hickerson, S.M.; Craft, N.; Beverley, S.M.; Wilson, M.E. In vivo imaging of transgenic *Leishmania* parasites in a live host. *J. Vis. Exp.* **2010**, 1980. [[CrossRef](#)]
17. Capul, A.A.; Barron, T.; Dobson, D.E.; Turco, S.J.; Beverley, S.M. Two functionally divergent UDP-Gal nucleotide sugar transporters participate in phosphoglycan synthesis in *Leishmania major*. *J. Biol. Chem.* **2007**, *282*, 14006–14017. [[CrossRef](#)] [[PubMed](#)]
18. Lara, D.; Feng, Y.; Bader, J.; Savage, P.B.; Maldonado, R.A. Anti-trypanosomatid activity of ceragenins. *J. Parasitol.* **2010**, *96*, 638–642. [[CrossRef](#)] [[PubMed](#)]
19. Khare, S.; Nagle, A.S.; Biggart, A.; Lai, Y.H.; Liang, F.; Davis, L.C.; Barnes, S.W.; Mathison, C.J.N.; Myburgh, E.; Gao, M.-Y.; et al. Proteasome inhibition for treatment of leishmaniasis, Chagas disease and sleeping sickness. *Nature* **2016**, *537*, 229–233. [[CrossRef](#)] [[PubMed](#)]
20. Schrödinger Suite 2018-1 Induced Fit Docking Protocol. Available online: <https://www.schrodinger.com/induced-fit> (accessed on 10 February 2018).

21. Clark, A.J.; Tiwary, P.; Borrelli, K.; Feng, S.; Miller, E.B.; Abel, R.; Friesner, R.A.; Berne, B.J. Prediction of Protein-Ligand Binding Poses via a Combination of Induced Fit Docking and Metadynamics Simulations. *J. Chem. Theory Comput.* **2016**, *12*, 2990–2998. [[CrossRef](#)] [[PubMed](#)]
22. Taylor, M.C.; Kelly, J.M.; Chapman, C.J.; Fairlamb, A.H.; Miles, M.A. The structure, organization, and expression of the *Leishmania donovani* gene encoding trypanothione reductase. *Mol. Biochem. Parasitol.* **1994**, *64*, 293–301. [[CrossRef](#)]
23. Tovar, J.; Wilkinson, S.; Mottram, J.C.; Fairlamb, A.H. Evidence that trypanothione reductase is an essential enzyme in *Leishmania* by targeted replacement of the tryA gene locus. *Mol. Microbiol.* **1998**, *29*, 653–660. [[CrossRef](#)] [[PubMed](#)]
24. Khan, M.O. Trypanothione reductase: A viable chemotherapeutic target for antitrypanosomal and antileishmanial drug design. *Drug Target Insights* **2007**, *2*, 129–146. [[CrossRef](#)] [[PubMed](#)]
25. Feasey, N.; Wansbrough-Jones, M.; Mabey, D.C.; Solomon, A.W. Neglected tropical diseases. *Br. Med. Bull.* **2010**, *93*, 179–200. [[CrossRef](#)] [[PubMed](#)]
26. Haidle, A.M.; Zabierek, A.A.; Childers, K.K.; Rosenstein, C.; Mathur, A.; Altman, M.D.; Chan, G.; Xu, L.; Bachman, E.; Mo, J.R.; et al. Thiophene carboxamide inhibitors of JAK2 as potential treatments for myeloproliferative neoplasms. *Bioorg. Med. Chem. Lett.* **2014**, *24*, 1968–1973. [[CrossRef](#)] [[PubMed](#)]
27. Huang, H.; Li, H.; Yang, S.; Chreifi, G.; Martasek, P.; Roman, L.J.; Meyskens, F.L.; Poulos, T.L.; Silverman, R.B. Potent and selective double-headed thiophene-2-carboximidamide inhibitors of neuronal nitric oxide synthase for the treatment of melanoma. *J. Med. Chem.* **2014**, *57*, 686–700. [[CrossRef](#)] [[PubMed](#)]
28. De Oliveira, J.F.; da Silva, A.L.; Vendramini-Costa, D.B.; da Cruz Amorim, C.A.; Campos, J.F.; Ribeiro, A.G.; de Moura, R.O.; Neves, J.L.; Ruiz, A.L.T.G.; de Carvalho, J.E.; et al. Synthesis of thiophene-thiosemicarbazone derivatives and evaluation of their in vitro and in vivo antitumor activities. *Eur. J. Med. Chem.* **2015**, *104*, 148–156. [[CrossRef](#)] [[PubMed](#)]
29. Marchais-Oberwinkler, S.; Xu, K.; Wetzel, M.; Perspicace, E.; Negri, M.; Meyer, A.; Odermatt, A.; Moller, G.; Adamski, J.; Hartmann, R.W. Structural Optimization of 2,5-Thiophene Amides as Highly Potent and Selective 17 beta-Hydroxysteroid Dehydrogenase Type 2 Inhibitors for the Treatment of Osteoporosis. *J. Med. Chem.* **2013**, *56*, 167–181. [[CrossRef](#)] [[PubMed](#)]
30. Opsenica, I.M.; Verbic, T.Z.; Tot, M.; Sciotti, R.J.; Pybus, B.S.; Djurkovic-Djakovic, O.; Slavic, K.; Solaja, B.A. Investigation into novel thiophene- and furan-based 4-amino-7-chloroquinolines afforded antimalarials that cure mice. *Bioorg. Med. Chem.* **2015**, *23*, 2176–2186. [[CrossRef](#)] [[PubMed](#)]
31. Patil, D.; Dash, R.P.; Thakur, S.K.; Pandya, A.N.; Venkatesh, P.; Vasu, K.K.; Nivsarkar, M. Implication of novel thiazolo-thiophene derivative (MCD-KV-10) for management of asthma. *J. Enzym. Inhib. Med. Chem.* **2015**, *30*, 229–239. [[CrossRef](#)] [[PubMed](#)]
32. Ghorab, M.M.; Al-Dhfyhan, A.; Al-Dosari, M.S.; El-Gazzar, M.G.; AlSaid, M.S. Antiproliferative activity of novel thiophene and thienopyrimidine derivatives. *Drug Res.* **2014**, *64*, 313–320. [[CrossRef](#)] [[PubMed](#)]
33. Ashok, P.; Lu, C.L.; Chander, S.; Zheng, Y.T.; Murugesan, S. Design, Synthesis, and Biological Evaluation of 1-(thiophen-2-yl)-9H-pyrido[3,4-b]indole Derivatives as Anti-HIV-1 Agents. *Chem. Biol. Drug Des.* **2015**, *85*, 722–728. [[CrossRef](#)] [[PubMed](#)]
34. Arango Duque, G.; Descoteaux, A. *Leishmania* survival in the macrophage: Where the ends justify the means. *Curr. Opin. Microbiol.* **2015**, *26*, 32–40. [[CrossRef](#)] [[PubMed](#)]
35. Butler, W.T. Pharmacology, toxicity, and therapeutic usefulness of amphotericin B. *JAMA* **1966**, *195*, 371–375. [[CrossRef](#)] [[PubMed](#)]
36. Amer, A.O.; Swanson, M.S. A phagosome of one's own: A microbial guide to life in the macrophage. *Curr. Opin. Microbiol.* **2002**, *5*, 56–61. [[CrossRef](#)]
37. Fonseca-Silva, F.; Inacio, J.D.F.; Canto-Cavaleiro, M.M.; Almeida-Amaral, E.E. Reactive oxygen species production and mitochondrial dysfunction contribute to quercetin induced death in *Leishmania amazonensis*. *PLoS ONE* **2011**, *6*, e14666. [[CrossRef](#)] [[PubMed](#)]
38. Lu, J.; Holmgren, A. The thioredoxin antioxidant system. *Free Radic. Biol. Med.* **2014**, *66*, 75–87. [[CrossRef](#)] [[PubMed](#)]
39. Irigoin, F.; Cibils, L.; Comini, M.A.; Wilkinson, S.R.; Flohe, L.; Radi, R. Insights into the redox biology of *Trypanosoma cruzi*: Trypanothione metabolism and oxidant detoxification. *Free Radic. Biol. Med.* **2008**, *45*, 733–742. [[CrossRef](#)] [[PubMed](#)]

40. Schmidt, A.; Krauth-Siegel, R.L. Enzymes of the trypanothione metabolism as targets for antitrypanosomal drug development. *Curr. Top. Med. Chem.* **2002**, *2*, 1239–1259. [[CrossRef](#)] [[PubMed](#)]
41. Wilkinson, S.R.; Horn, D.; Prathalingam, S.R.; Kelly, J.M. RNA interference identifies two hydroperoxide metabolizing enzymes that are essential to the bloodstream form of the african trypanosome. *J. Biol. Chem.* **2003**, *278*, 31640–31646. [[CrossRef](#)] [[PubMed](#)]
42. Martinez, A.; Carreon, T.; Iniguez, E.; Anzellotti, A.; Sanchez, A.; Tyan, M.; Sattler, A.; Herrera, L.; Maldonado, R.A.; Sanchez-Delgado, R.A. Searching for new chemotherapies for tropical diseases: Ruthenium-clotrimazole complexes display high in vitro activity against *Leishmania major* and *Trypanosoma cruzi* and low toxicity toward normal mammalian cells. *J. Med. Chem.* **2012**, *55*, 3867–3877. [[CrossRef](#)] [[PubMed](#)]
43. Capul, A.A.; Hickerson, S.; Barron, T.; Turco, S.J.; Beverley, S.M. Comparisons of mutants lacking the Golgi UDP-galactose or GDP-mannose transporters establish that phosphoglycans are important for promastigote but not amastigote virulence in *Leishmania major*. *Infect. Immun.* **2007**, *75*, 4629–4637. [[CrossRef](#)] [[PubMed](#)]
44. Lema, C.; Varela-Ramirez, A.; Aguilera, R.J. Differential nuclear staining assay for high-throughput screening to identify cytotoxic compounds. *Curr. Cell. Biochem.* **2011**, *1*, 1–14. [[PubMed](#)]
45. Iniguez, E.; Sanchez, A.; Vasquez, M.A.; Martinez, A.; Olivas, J.; Sattler, A.; Sanchez-Delgado, R.A.; Maldonado, R.A. Metal-drug synergy: New ruthenium(II) complexes of ketoconazole are highly active against *Leishmania major* and *Trypanosoma cruzi* and nontoxic to human or murine normal cells. *J. Biol. Inorg. Chem.* **2013**, *18*, 779–790. [[CrossRef](#)] [[PubMed](#)]
46. Baiocco, P.; Colotti, G.; Franceschini, S.; Ilari, A. Molecular basis of antimony treatment in leishmaniasis. *J. Med. Chem.* **2009**, *52*, 2603–2612. [[CrossRef](#)] [[PubMed](#)]
47. Halgren, T. New method for fast and accurate binding-site identification and analysis. *Chem. Biol. Drug Des.* **2007**, *69*, 146–148. [[CrossRef](#)] [[PubMed](#)]

Sample Availability: Samples of the compounds are not available from the authors.



© 2018 by the authors. Licensee MDPI, Basel, Switzerland. This article is an open access article distributed under the terms and conditions of the Creative Commons Attribution (CC BY) license (<http://creativecommons.org/licenses/by/4.0/>).